

# The influence of bicuspid aortic valves on the dynamic pressure distribution in the ascending aorta: a porcine *ex vivo* model<sup>†</sup>

Andrzej Juraszek<sup>a,b,c</sup>, Tomasz Dziudzio<sup>a,b</sup>, Martin Stoiber<sup>a,b</sup>, Daniel Fechtig<sup>a</sup>, Verena Gschlad<sup>a,b</sup>, Philipp Aigner<sup>a,b</sup>,  
Martin Czerny<sup>d,\*</sup> and Heinrich Schima<sup>a,b,e</sup>

<sup>a</sup> Center for Medical Physics and Biomedical Engineering, Vienna, Austria

<sup>b</sup> Ludwig-Boltzmann-Cluster for Cardiovascular Research, Vienna, Austria

<sup>c</sup> Department of Cardiac Surgery and Transplantation, The Cardinal Stefan Wyszyński Institute of Cardiology, Warsaw, Poland

<sup>d</sup> Department of Cardiovascular Surgery, University Hospital Berne, Berne, Switzerland

<sup>e</sup> Department of Cardiac Surgery, Medical University, Vienna, Austria

\* Corresponding author. Freiburgstrasse, 3010 Berne, Switzerland. Tel: +41-31-6322111; fax: +41-31-6329019; e-mail: martin.czerny@insel.ch (M. Czerny).

Received 15 July 2013; received in revised form 24 November 2013; accepted 3 December 2013

## Abstract

**OBJECTIVES:** The aim of the study was to simulate the effect of different bicuspid aortic valve configurations on the dynamic pressure distribution in the ascending aorta.

**METHODS:** Aortic specimens were harvested from adult domestic pigs. In Group 1, bicuspidalization was created by a running suture between the left and the right coronary leaflets ( $n = 6$ ) and in Group 2 by a running suture between the left and the non-coronary leaflets ( $n = 6$ ). Eleven tricuspid specimens served as controls. Two intraluminal pressure catheters were positioned at the concavity and the convexity of the ascending aorta. The specimens were connected to a mock circulation (heart rate: 60 bpm, target pressure: 95 mmHg). A comparison of the different conditions was also done in a numerical simulation.

**RESULTS:** At a distal mean aortic pressure of  $94 \pm 10$  mmHg, a mean flow rate of  $5.2 \pm 0.3$  l/min was achieved. The difference of maximal dynamic pressure values (which occurred in systole) between locations at the convexity and the concavity was  $7.8 \pm 2.9$  mmHg for the bicuspid and  $1.0 \pm 0.9$  mmHg for the tricuspid specimens ( $P < 0.001$ ). The numerical simulation revealed an even higher pressure difference between convexity and concavity for bicuspid formation.

**CONCLUSIONS:** In this hydrodynamic mock circulation model, we were able to demonstrate that bicuspid aortic valves are associated with significant pressure differences in different locations within the ascending aorta compared with tricuspid aortic valves. These altered pressure distributions and flow patterns may further add to the understanding of aneurysmal development in patients with bicuspid aortic valves and might serve to anticipate adverse aortic events due to a better knowledge of the underlying mechanisms.

**Keywords:** Bicuspid aortic valve • Circulation model • Aneurysm • Haemodynamics • Dynamic pressure

## INTRODUCTION

A bicuspid aortic valve is a common congenital heart defect and strongly associated with ascending aortic aneurysm formation [1–3]. Although in the last few years the haemodynamic theory of aortic dilatation in patients with a bicuspid aortic valve seemed to be discounted by the theory of intrinsic aortic wall weakness, some recent publications suggest that the process of aortic dilatation is caused both by aortic wall pathologies and by abnormal haemodynamics [4–6]. It is known that bicuspid aortic valves may cause a high-speed jet-shaped flow, which results in high flow velocities in the vicinity of the ascending aortic wall [7]. In consequence, the wall shear stress is massively increased.

Furthermore, in case of an irregularity developing within the wall, for example a starting lesion, parts of the jet flow are stopped by this irregularity leading to a conversion of kinetic energy into static pressure. This is basically described by the equation of Bernoulli [8]:

$$P_{\text{total}} = P_{\text{stat}} + P_{\text{grav}} + P_{\text{dyn}} = P_{\text{stat}} + \rho g H + \rho v^2 / 2$$

where  $P_{\text{total}}$  is the overall total sum of pressure,  $P_{\text{stat}}$  the static pressure (in our case the time-varying aortic pressure) and  $P_{\text{dyn}}$  the dynamic pressure due to the kinetic energy of the moving blood.  $P_{\text{grav}}$  is calculated from the product of density  $\rho$ , gravity constant  $g$  and height difference  $H$  between the measurement location and the actual point (negligible in the aspects discussed here).  $P_{\text{dyn}}$  is calculated from blood density  $\rho$  and the square of the local blood velocity  $v$ . In the normal circulation, dynamic pressure would be

<sup>†</sup>Presented at the 27th Annual Meeting of the European Association for Cardio-Thoracic Surgery, Vienna, Austria, 5–9 October 2013.

rather negligible, compared with static pressure. In stenotic geometries, however, in which local velocity increases to several metres per second, dynamic pressure can grow to the same order of magnitude as the static pressure, due to the quadratic influence of velocity.

The aim of the study was, therefore, to investigate the influence of bicuspid aortic valves on these velocity jets and the resulting dynamic pressure distribution in the ascending aorta in an experimental *ex vivo* model and the validation of these tests in a numerical simulation.

## MATERIALS AND METHODS

Two complementary approaches were chosen. First, an experimental model based on an already established preparation of porcine aortas was used to measure the dynamic pressures exerted by normal aortic valves and valves modified to bicuspid opening characteristics. Afterwards, a numerical model was implemented to validate the experimental results and further to determine wall shear stress and wall tension, which were not accessible in the experimental setting.

### Experimental model: preparing of aortic specimens

Segments of the thoracic aorta consisting of the aortic root to the mid descending aorta were harvested from adult domestic pigs. The pig aortas used were obtained from a European Union-certified slaughterhouse. As such, animals were not sacrificed specifically for this study. The aortas were then washed with cold water and transported in a water container directly to the laboratory. The time between harvesting and start of preparation was ~30–60 min. The porcine aorta is a good equivalent of the human aorta showing similar wall elasticity and anatomy. In every aortic specimen origins of coronary and intercostal arteries were closed using a 5.0 suture (Prolene®). We used an established classification of BAV in our experimental setting [9]. For constructing the

bicuspid valve 3 two-stitch pledgeted 5.0 sutures were used for each aortic specimen. The function of the created bicuspid valve was proved by an endoscope camera (Storz®) (Fig. 1). In 6 cases bicuspidalization was created between the left and the right coronary leaflets (Type 1). In another 6 cases bicuspidalization was created between the left and the non-coronary leaflets (Type 2). We did not go for the third type of bicuspidalization as we felt that for the proof of principle the two variants used were sufficient.

Two pressure catheters (Hellige®, Freiburg, Germany) were inserted via the supra-aortic branches and sewn to the aortic wall on the convexity and concavity in the mid ascending aorta (Figs 2 and 3). After the measurements in the mock circulation described below, the bicuspidalization sutures were removed and further measurements were done in the regular tricuspid setting (NT) ( $n = 11$ ).

### Experimental set-up

As previously described, the circulation was driven by a pneumatically driven Vienna heart pump to mimic aortic flow and pressure [10–12]. A rubber tube, a damping fibre element and an adjustable resistor mimicked peripheral arterial impedance (Fig. 4). The aortic annulus was sewn into a silicon ring of a driving chamber and the distal aorta was connected to a tube with adjustable resistance elements. Water was chosen as test fluid due to the unavoidable leakages of the preparation and the consequent necessity for continuous refill. In the numerical model (described below) it was proved that the difference in test fluid viscosity compared with blood was negligible for the results of dynamic pressure and the jet effects. After insertion of the aorta, the system was filled and deaired, and the circulation was started with a pumping frequency of 60 bpm. Pressure was steadily elevated using peripheral resistant elements to a target mean pressure of at least 90 mmHg at flow rates of at least 4.8 l/min. Under stable conditions data were recorded using pressure catheters (pnb®, Critical Care GmbH, Kirchseeon, Germany) and a custom-made Matlab® recording

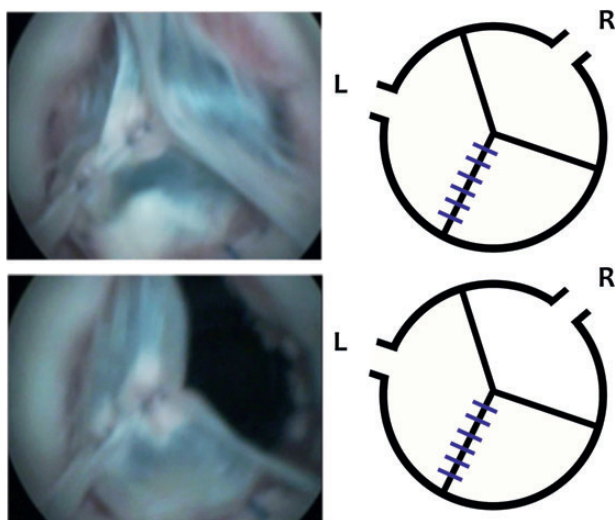


**Figure 1:** Endoscopic view of an artificially created bicuspid aortic valve. (A) Diastolic position, (B) systolic position. L: origin of the left coronary artery; R: origin of the right coronary artery.

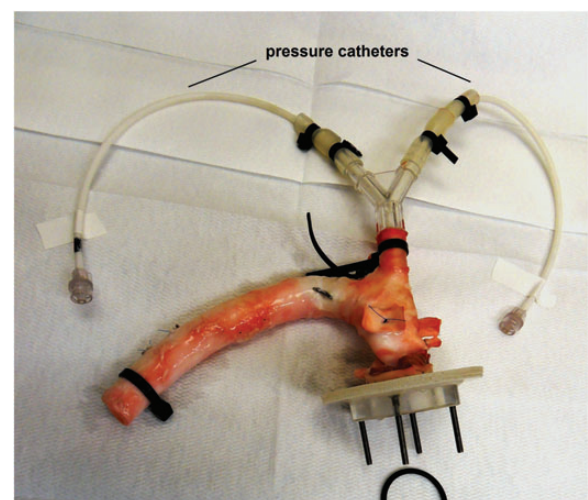


**Figure 2:** A prepared specimen with two pressure catheters installed.

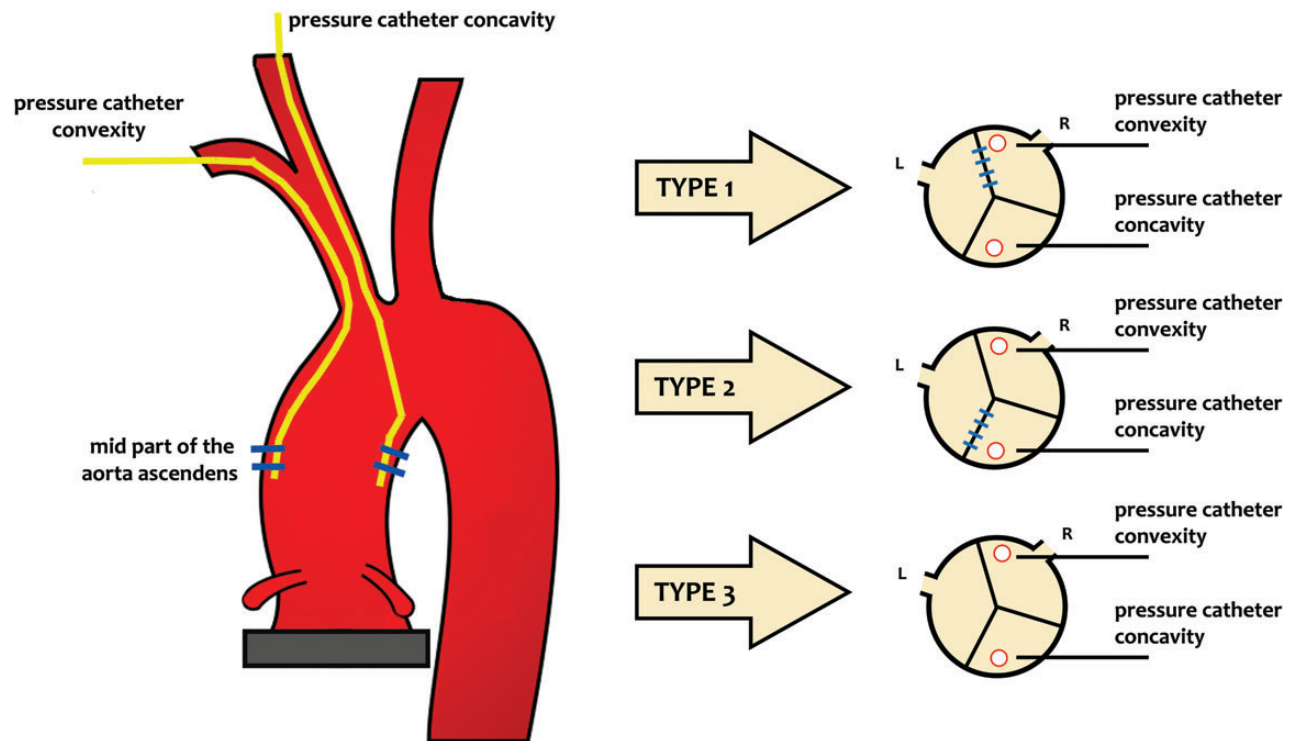


**Figure 3:** Pressure catheters and valve configurations. The raphe between the sewn aortic valve leaflets are marked blue. L: origin of the left coronary artery; R: origin of the right coronary artery.

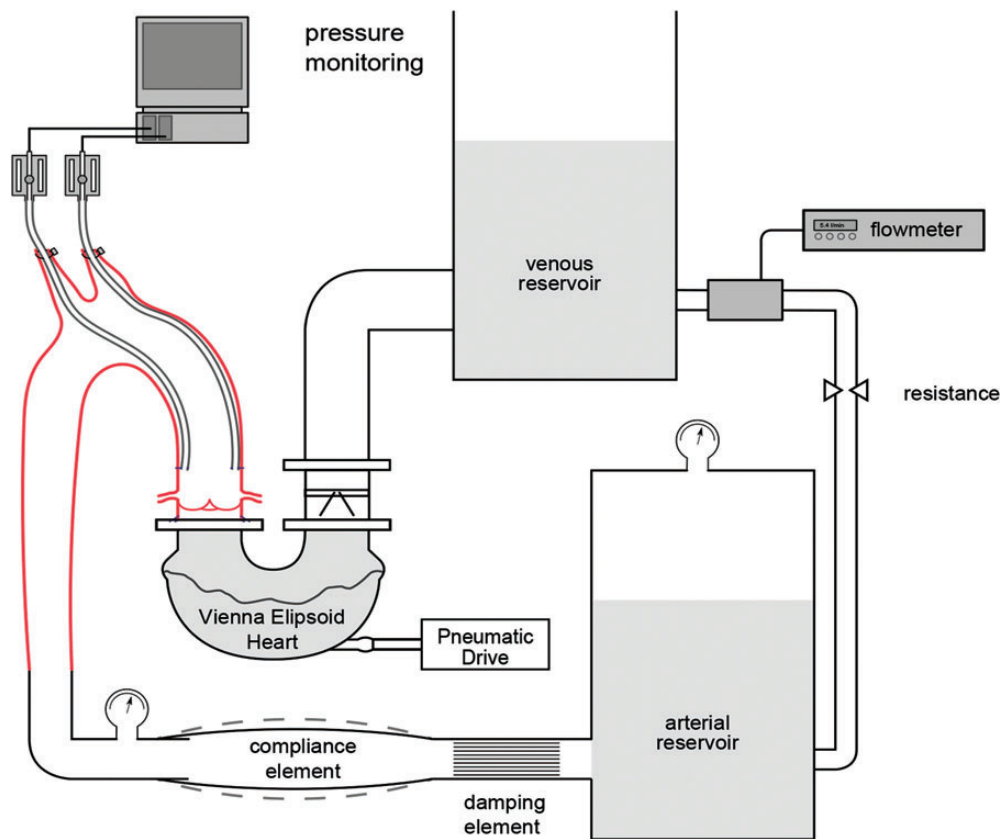


**Figure 4:** Mock circulation with aorta.

**Table 1:** Registered flow and pressure values

Valve type	Type 1—left/right coronary bicuspid (mean $\pm$ SD)	Type 2—left/non-coronary bicuspid (mean $\pm$ SD)	NT—tricuspid (mean $\pm$ SD)
Number of specimens	6	6	11
Mean flow (l/min)	5.34 $\pm$ 0.32	5.14 $\pm$ 0.21	5.19 $\pm$ 0.25
Mean pressure convexity (mmHg)	109.55 $\pm$ 13.91	95.34 $\pm$ 10.94	97.34 $\pm$ 7.78
Diastolic pressure convexity (mmHg)	81.23 $\pm$ 15.69	62.03 $\pm$ 13.37	64.60 $\pm$ 9.59
Systolic pressure convexity (mmHg)	156.96 $\pm$ 18.46	156.55 $\pm$ 9.16	159.98 $\pm$ 8.27
Mean pressure concavity (mmHg)	111.74 $\pm$ 14.35	93.92 $\pm$ 10.35	99.19 $\pm$ 7.75
Diastolic pressure concavity (mmHg)	81.23 $\pm$ 15.69	62.89 $\pm$ 11.70	66.59 $\pm$ 9.37
Systolic pressure concavity (mmHg)	163.56 $\pm$ 19.50	147.65 $\pm$ 9.93	158.63 $\pm$ 8.58
Absolute difference between maximum convexity and concavity (mmHg)	6.59 $\pm$ 2.08	8.90 $\pm$ 3.22	0.95 $\pm$ 0.85

Software. The peripheral pressure in the aorta, the dynamic pressure in the pressure catheters as well as the circulatory flow were recorded for 30 s.

### Statistical analysis

Data are reported as mean  $\pm$  SD. The absolute difference between the pressures of the two pressure catheters was calculated for each measurement. This maximum difference occurred approximately in the peak of systole. After testing for normality of distribution, Student's *t*-test was performed using the SPSS 17 software (SPSS, Inc, Chicago, IL, USA). A two-sided *P*-value of  $<0.05$  was considered statistically significant.

### Numerical study

To validate the experimental results, the flow distribution in the human aorta was numerically assessed for the normal tricuspid situation and the previously described two bicuspid aortic valve geometries (Type 1 and Type 2).

A numerical stiff grid model of the ventricular outflow tract, the open aortic valve and the aortic arch was digitized with 1.5 million cells. The orifice area of the bicuspid outflow tract was designed as a converging ellipse with diameters of 12 mm (major axis) and 10 mm (minor axis). The ascending aorta was geometrically designed as a bending and tapering tube with a maximum diameter of  $\sim 21$  mm. Blood was assumed to be a Newtonian liquid (constant viscosity), considering a mass density of  $1050 \text{ kg/m}^3$  and a viscosity of  $0.0035 \text{ Pa s}$ . The pulsatile inlet profile used in the experimental set-up was digitized to serve as an inflow boundary condition. To attain the conditions of the experimental set-up, the cross sections of carotid artery, subclavian artery and brachiocephalic trunk were considered occluded. The cross section of the abdominal aorta was defined as a static pressure outlet (pressure set to 0 Pa). Highly narrowed orifice areas support the onset of turbulent blood flow. To account for the probable onset of turbulent blood flow, heavily supported by narrowed orifice areas, turbulence modelling (Transition-SST- $k-\omega$ -solver of ANSYS®) was performed.

Besides the global velocity distribution, jet velocity and wall pressure were calculated. To take even the effect of the catheters

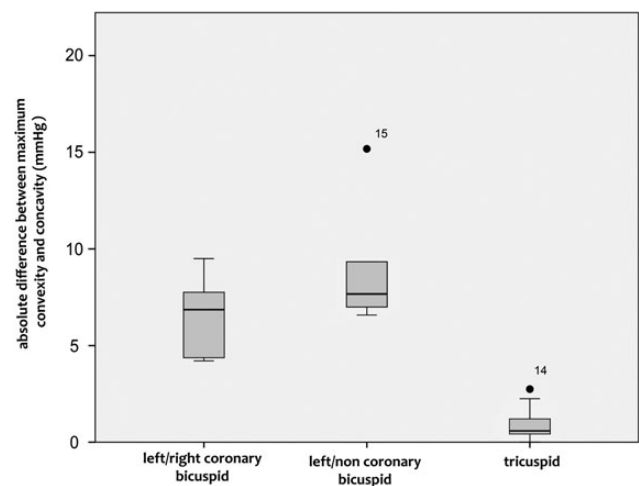


**Figure 5:** A box plot diagram comparing the pressure values between the three valve types.

in the *in vitro* setting into account, they were modelled as located in the symmetry plane of the aortic geometry.

## RESULTS

### Experimental model: general circulatory parameters

The mean peripheral pressure value was  $94 \pm 10$  mmHg, the mean of minimal diastolic pressures  $77 \pm 11$  mmHg and the mean of maximal systolic pressures  $115 \pm 10$  mmHg in 30 s registration time. The mean flow was  $5.2 \pm 0.3$  l/min. Values for each valve type are given in Table 1.

### Total pressure values in the ascending aorta

Results are given in Table 1. The following total pressure values were recorded in the Type 1 setting: maximal total pressure on the convexity was  $157 \pm 18$  mmHg and  $164 \pm 20$  mmHg on the concavity. The Type 2 setting showed the following parameters:



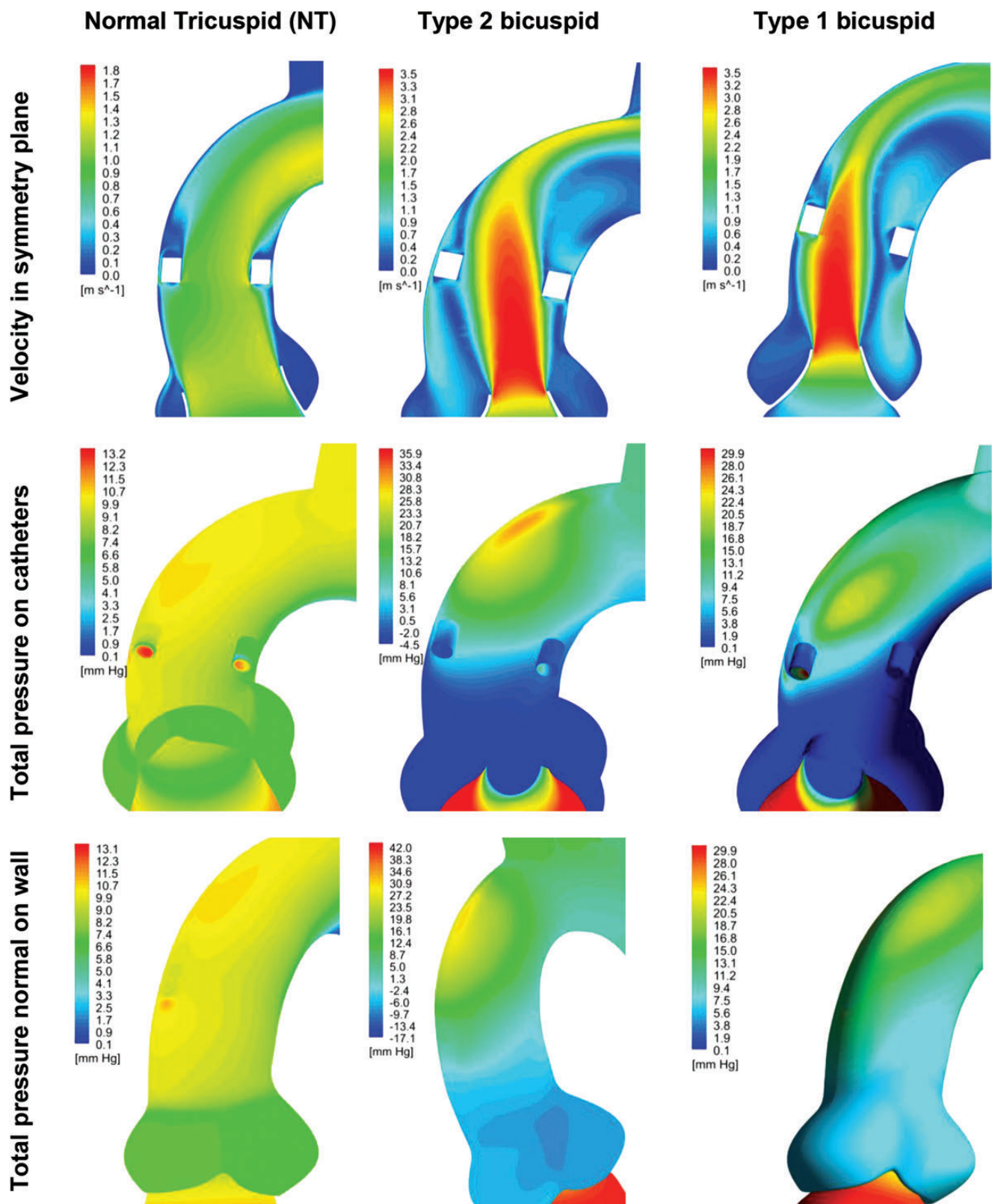


Figure 6: CFD blood flow simulations in the ascending portion of the aorta. Comparison of velocity and total pressure in healthy tricuspid (NT), Type 2 and Type 1 bicuspid configurations. For simplicity, the thoracic and abdominal part of the aorta is not shown. Mind that the colour bars are individual for each simulation.

maximal total pressure on the convexity was  $157 \pm 9$  mmHg and  $148 \pm 10$  mmHg on the concavity. The NT setting showed values listed: maximal total pressure on the convexity was  $160 \pm 8$  mmHg and  $159 \pm 9$  mmHg on the concavity. The absolute difference in maximal total pressure between convexity and concavity of the aorta was significantly higher in the bicuspid aortic valve group ( $8 \pm 3$  mmHg) than in the tricuspid aortic valve group ( $1.0 \pm 0.9$  mmHg) ( $P < 0.001$ ). A comparison of these values is shown in Fig. 5.

### Numerical study: dynamic and total pressure values *in silico*

Via an approximate averaging of pressure values on the surface of each catheter, pressure differences between convexity and concavity were calculated. Whereas a pressure difference of 2 mmHg in the tricuspid case is moderate, simulations in the Type 2 and Type 1 bicuspid cases revealed pressure differences of at least 8–10 and 20 mmHg, respectively (Fig. 6). Depending on the angle of incidence, the orifice area and the cross-sectional location of the bicuspid valve and location of the catheters, even higher jet velocities yielding higher pressure differences could be provoked in the simulation.

## DISCUSSION

As generally known, aortic valve pathology of various kinds may lead to altered haemodynamic patterns and therefore aortic wall stress distributions in the ascending aorta. Depending on the location and shape of the valve pathology, such jets can be directed either axially and then decelerated in the fluid or towards the aortic wall, causing a considerable elevation of wall shear stress [13]. The dynamic energy in blood increases with the square of velocity, which in case of wall irregularities or obstacles such as atherosclerotic plaque formations or other structural aortic wall disease may be converted into relevant static pressure respectively force. Whereas our experimental trial specimens with normal tricuspid configuration (NT) did not cause jets and did, as expected, not show a difference in dynamic pressure values between the convexity and the concavity of the aorta, bicuspid valves increased the maximal dynamic and therefore also the total pressure above the orifice of the aortic valve. These different pressure distributions near the aortic wall can cause heterogeneous flow patterns in the ascending aorta and may enhance the process of the aortic wall deterioration, especially in patients with inherent aortic wall disease.

The *in silico* numerical model was used to provide a conclusive scheme of the jet shape and to study the pressure effects of parameter variations under fixed boundary conditions. The model was kept intentionally simple (with fixed valve geometry and without elasticity effects). The pressure difference between convexity and concavity calculated in the numerical model agreed well with the experimental data—the effect even exceeded the experimentally shown phenomena. The relation between catheter position and pressure difference might be altered by many factors: eventual asymmetries of the jet positioned between the inner or outer aortic wall, the curvature of the wall, the aortic diameter and the orientation of the valve.

Further, it could be shown in simulations that with more extreme geometric assumptions in jet angle up to a threefold higher pressure difference between inner and outer circumference could be possible. With the given *in vitro* setting, however, a quantitative validation of such extreme conditions was achieved. However, qualitatively both methods show the effects of stenotic valve orifice area on the blood pressure distribution apparent in the ascending aorta.

Blood flow at the convexity may be hindered by developing lesions of the aortic wall, which in turn transforms dynamic pressure of the blood stream into static pressure acting onto disintegrated aortic tissue. An increased blood pressure in these regions, therefore, may be a potent factor for further development and propagation of the lesion, leading to aortic dissection and ascending aortic aneurysm. Higher blood pressure at the convexity of the ascending aortic wall leads to higher mechanical wall load in this region, which may influence accelerated tissue weakening processes. In case of already existing lesions, the elevated stagnation pressure would promote aortic dissections and subsequent aneurysms.

The main intention behind this study was to develop a better understanding of haemodynamic factors behind associated ascending aortic disease in bicuspid aortic valves. By bicuspidalizing tricuspid porcine aortic valves we simulated the two forms of bicuspid aortic valves with a raphe [14]. Interestingly, even this small effect was able to create significant pressure differences between the concavity and the convexity of the ascending aorta. So it might well be anticipated that when aortic valve disease progresses, the associated gradients across the valve might accelerate and perpetuate this mechanism.

A further important finding was that by increasing angulation of the ascending aorta in the numerical simulation, the pressure difference between concavity and convexity could be amplified. This is important as clinical observations do confirm that in acute aortic dissections angulation between the left ventricular outflow tract and the ascending aorta is more pronounced as it is the case in bicuspid aortic valves *per se* [15]. As a clinical consequence of our work, a stronger focus on parameters not having been decisive to date could be implemented. Furthermore, when non-invasive blood pressure measurements become routine, this approach might be helpful in identifying patients at risk of rapid progression of their ascending aortic pathology or the ones being at risk of acute aortic dissection. On the other hand, our findings have to be seen as they are, namely an experimental approximation of clinical situations that cannot be transferred into clinics in a one-to-one fashion. The main reason is the fact that the diversity and its reason for bicuspid aortic valves are numerous and a definite differentiation between inherited and haemodynamic reasons for ascending aortic dilatation is illusive.

### Limitations of the study

This study encompasses of course all advantages, but also limitations of an *ex vivo* experimental study. Our experiment and the circulatory set-up are an approximation of the human blood circulation system, with highly reproducible flow conditions, but limited accuracy of the compliance of the outflow vessels, particularly the brachiocephalic trunk, which may lead to a minor exaggeration of pressure peaks. On the other hand, the use of a natural aorta with its natural elasticity did enormously reduce water

hammer effects seen in stiff wall systems [16]. The used test fluid is non-Newtonian, which however has no relevant influence in the high-speed conditions of the aorta [17]. The experimental *ex vivo* model has its own limitations regarding the precision of the measurements. In our opinion, a comparison of the different bicuspid valve types would not deliver objective results. The detected pressure difference between the two common bicuspid valve types may be affected too much by the experimental set-up. We decided to include the rare BAV fusion into our study to avoid the inappropriate comparison between the most common BAV types. Further, the numerical model, which was used for validation of the experimental results, was kept rather simple to fit to the limited available computer power: The model assumed non-moving valve leaflets, a stiff wall and an axisymmetric behaviour. This was considered certainly sufficient to prove the experiments, but should not be used *per se* for excessive interpretations of the aortic flow. The numerical results are provided as support of the *in vitro* model and the quality of the effect, not for absolute quantitative numbers.

Summarizing, in this hydrodynamic mock circulation model, we were able to demonstrate that bicuspid aortic valves are associated with significant pressure differences in different locations within the ascending aorta when compared with tricuspid aortic valves. These altered pressure distributions and, consecutively, flow patterns may further add to the understanding of aneurysmal development in patients with bicuspid aortic valves and might serve to anticipate adverse aortic events due to a better knowledge of the underlying mechanisms.

**Conflict of interest:** none declared.

## REFERENCES

- [1] Yener N, Oktar GL, Erer D, Yardimci MM, Yener A. Bicuspid aortic valve. *Ann Thorac Cardiovasc Surg* 2002;8:264–7.
- [2] Hahn RT, Roman MJ, Mogtader AH, Devereux RB. Association of aortic dilation with regurgitant, stenotic and functionally normal bicuspid aortic valves. *J Am Coll Cardiol* 1992;19:283–88.
- [3] Keane MG, Wieggers SE, Plappert T, Pochettino A, Bavaria JE, Sutton MG. Bicuspid aortic valves are associated with aortic dilatation out of proportion to coexistent valvular lesions. *Circulation* 2000;102:III35–39.
- [4] Fedak PWM, Verma S, David TE, Leask RL, Weisel RD, Butany J. Clinical and pathophysiological implications of a bicuspid aortic valve. *Circulation* 2002;106:900–4.
- [5] Coady MA, Sellke FW. Metallothionein link to bicuspid aortic valve-associated ascending aortic dilatation. *Circulation* 2009;119:2423–5.
- [6] Bauer M, Siniawski H, Pasic M, Schaumann B, Hetzer R. Different hemodynamic stress of the ascending aorta wall in patients with bicuspid and tricuspid aortic valve. *J Card Surg* 2006;21:218–20.
- [7] Viscardi F, Vergara C, Antiga L, Merelli S, Veneziani A, Puppini G et al. Comparative finite element model analysis of ascending aortic flow in bicuspid and tricuspid aortic valve. *Artif Organs* 2010;34:1114–20.
- [8] Milnor W. *Cardiovascular Physiology*. New York, NY: Oxford University Press, 1990, 182–4.
- [9] Schaefer M, Lewin MB, Stout KK, Gill E, Prueitt A, Byers PH et al. The bicuspid aortic valve: an integrated phenotypic classification of leaflet morphology and aortic root shape. *Heart* 2008;94:1634–8.
- [10] Schima H, Baumgartner H, Spitaler F, Kuhn P, Wolner E. A modular mock circulation for hydromechanical studies on valves, stenoses, vascular grafts and cardiac assist devices. *Int J Artif Organs* 1992;15:417–21.
- [11] Zimpfer D, Schima H, Czerny M, Kasimir MT, Sandner S, Seebacher G et al. Experimental stentgraft treatment of ascending aortic dissection. *Ann Thorac Surg* 2008;85:470–3.
- [12] Trubel W, Losert U, Schima H, Rokitsky A, Spiss CK, Coraim F et al. Total artificial heart bridging: a temporary support for deteriorating heart transplantation-candidates—methods and results. *Thorac Cardiovasc Surg* 1987;35:277–82.
- [13] Barker AJ, Lanning C, Shandas R. Quantification of hemodynamic wall shear stress in patients with bicuspid aortic valve using phase-contrast MRI. *Ann Biomed Eng* 2010;38:788–800.
- [14] Sievers HH, Schmidtke C. A classification system for the bicuspid aortic valve from 304 surgical specimens. *J Thorac Cardiovasc Surg* 2007;133:1226–33.
- [15] Den Reijer PM, Sallee D III, van der Velden P, Zaaijer ER, Parks WJ, Ramamurthy S et al. Hemodynamic predictors of aortic dilatation in bicuspid aortic valve by velocity-encoded cardiovascular magnetic resonance. *J Cardiovasc Magn Reson* 2010;12:4.
- [16] Simon-Kupilik N, Schima H, Huber L, Moidl R, Wipplinger G, Losert U et al. Prosthetic replacement of the aorta is a risk factor for aortic root aneurysm development. *Ann Thorac Surg* 2002;73:455–9.
- [17] Liu X, Fan Y, Deng X, Zhan F. Effect of non-Newtonian and pulsatile blood flow on mass transport in the human aorta. *J Biomech* 2011;44:1123–31.

## APPENDIX. CONFERENCE DISCUSSION

**Dr E. Girdauskas (Bad Berka, Germany):** Dr Juraszek and coauthors have performed this research in order to better define the role of haemodynamics in bicuspid aortopathy. The authors implemented two complementary models in order to analyse the distribution of dynamic pressure in the convexity versus concavity of the ascending aorta. Two different fusion forms of bicuspid valve were analysed with the regular tricuspid valve serving as a control. Both models consistently demonstrated a markedly uneven pressure distribution between concavity and convexity of the ascending aorta in the setting of bicuspid aortic valve as opposed to the tricuspid control. Moreover, this uneven pressure distribution was influenced by the fusion type of bicuspid aortic valve and the angulation between the left ventricular outflow tract and the ascending aorta. Whilst taking into account all the limitations of the experimental model which have been adequately addressed by the authors, these data demonstrate convincingly the role of flow-induced vascular remodelling in the development of bicuspid aortopathy. These results are in line with the recent rheological studies published by others.

My comments are intended only to add some details to this excellent study. First of all, different aortic dilatation patterns have been advocated in distinct bicuspid aortic valve fusion forms, as observed in surgical and echocardiographic follow-up studies. Larger root dimensions have been advocated in bicuspid patients with right and left coronary cusp fusion, whereas increased aortic arch diameters have been shown in right and noncoronary fusion. What do the authors think about this finding? Would the mock circulation model, as implemented in this study, allow for analysis of different aortic dilatation patterns in distinct bicuspid geometries? For this purpose, I think inclusion of right and nonfusion pattern, which is known to be the second most common geometric configuration of bicuspid valve, seems to me reasonable.

And secondly, the authors noticed that pressure difference between concavity and convexity could be exaggerated by modelling the angle of flow jet, the orifice area, and the geometric orientation of the bicuspid valve. Could the authors share some details with us on that issue and especially which geometric configuration of bicuspid valve was associated with the highest pressure difference between the inner and outer curvature. Did the authors observe a direct linear correlation between the decreasing orifice area of the bicuspid valve and the pressure difference between convexity and concavity?

**Dr Juraszek:** First, I would like to answer the question regarding the *ex vivo* model and the difference between the different types of bicuspid valves. As you know, working with an *ex vivo* porcine model has its borders. And in the beginning we tried to compare all these types of bicuspid valves and we also performed some cases of the right noncoronary valves. We came to the conclusion that this circulatory model was going too far and would not in fact achieve objective results. The only thing we were going to measure was the general difference between the tricuspid valves and the bicuspid valves. We think that the anatomy of the pig aorta, and especially of the pig aortic root, differs slightly from the human one. Finally, the size of the pressure-measuring catheters may influence this comparison and lead to a bias. Indeed, we tried it and we did not go further because we did not want to publish numbers which have a chance of bias.

The situation was similar for the numerical simulation. If the position of the orifice area is changed, the direction of the jet in the ascending aorta is changed too. If we would perform a more complex computer simulation and take into account different positions of the orifice area and different angles of the ascending aorta, we would achieve a more significant difference in the pressure residing in the ascending aorta. In the end, a more detailed study is necessary, including another experimental setup to further elaborate on this study.